

Lawrence Berkeley National Laboratory

Recent Work

Title

A FINITE ELEMENT METHOD FOR THE STUDY OF SOLIDIFICATION PROCESSES IN THE PRESENCE OF NATURAL CONVECTION

Permalink

<https://escholarship.org/uc/item/8hw1b221>

Authors

Yoo, J.
Rubinsky, B.

Publication Date

1984-09-01

LBL-19275
c.2

LBL-19275
Preprint

RECEIVED
LAWRENCE
BERKLEY LABORATORY

APR 17 1985

LIBRARY AND
DOCUMENTS SECTION

Submitted to the
International Journal for
Numerical Methods in
Engineering

A FINITE ELEMENT METHOD
FOR THE STUDY OF
SOLIDIFICATION PROCESSES
IN THE PRESENCE OF
NATURAL CONVECTION

J. Yoo and B. Rubinsky

September 1984

CAM

TWO-WEEK LOAN COPY

*This is a Library Circulating Copy
which may be borrowed for two weeks.*

Lawrence Berkeley Laboratory
University of California
Berkeley, California 94720

Prepared for the U.S. Department of Energy
under Contract DE-AC03-76SF00098

**Center
for
Advanced
Materials**

LBL-19275
c.2

DISCLAIMER

This document was prepared as an account of work sponsored by the United States Government. While this document is believed to contain correct information, neither the United States Government nor any agency thereof, nor the Regents of the University of California, nor any of their employees, makes any warranty, express or implied, or assumes any legal responsibility for the accuracy, completeness, or usefulness of any information, apparatus, product, or process disclosed, or represents that its use would not infringe privately owned rights. Reference herein to any specific commercial product, process, or service by its trade name, trademark, manufacturer, or otherwise, does not necessarily constitute or imply its endorsement, recommendation, or favoring by the United States Government or any agency thereof, or the Regents of the University of California. The views and opinions of authors expressed herein do not necessarily state or reflect those of the United States Government or any agency thereof or the Regents of the University of California.

A Finite Element Method for the Study of Solidification
Processes in the Presence of Natural Convection

by

Jaisuk Yoo
Research Associate

B. Rubinsky*
Associate Professor

Center for Advanced Materials
Lawrence Berkeley Laboratory

and

Department of Mechanical Engineering
University of California at Berkeley
Berkeley, CA 94720, U.S.A.

*

To whom the correspondence should be addressed.

Summary

A new numerical technique was developed for the analysis of two-dimensional transient solidification processes in the presence of time dependent natural convection in the melt. The method can cope with irregular, transient morphologies of the solid-liquid interface using a new Galerkin formulation for the energy balance on the solid-liquid interface. The finite element solution to the Galerkin formulation yields the displacement of individual nodes on the solid-liquid interface. The displacement of the nodes is expressed by uncoupled components in the x and y direction.

The fluid flow problem was solved using a "penalty" formulation. Numerical experiments were performed for Rayleigh numbers as high as 10^6 to demonstrate the method and to indicate the effect of natural convection on the solid-liquid interface morphology.

Nomenclature

<u>A</u>	conductivity matrix
<u>B</u>	spacial gradient matrix
<u>B</u> _{1,2}	spacial gradient in x and y direction
<u>C</u> _{11,22}	convection matrix
<u>c</u> _p	heat capacity
<u>c</u> _{1,2}	coefficient
<u>g</u>	gravity
<u>H</u>	interpolation matrix
<u>H</u> _{s1}	latent heat
<u>H</u>	aspect ratio
<u>h</u> _i	interpolation function
<u>J</u>	Jacobian operator
<u>J</u>	Jacobian
<u>K</u>	conductivity matrix
<u>k</u>	conductivity
<u>L</u> _{ph}	latent heat matrix
<u>L</u>	coefficient matrix of penalty term
<u>L</u>	characteristic length
<u>M</u>	capacity matrix
<u>n</u>	normal vector
<u>n</u>	normal direction
<u>P</u>	point
<u>P</u> _d	dynamic pressure
<u>Pr</u>	Prandtl number

\underline{Q}	heat flux matrix
q	normal heat flux
R	region of discussion
R_k	ratio of thermal conductivity
R_α	ratio of thermal diffusivity
\underline{R}	force matrix
Ra	Rayleigh number
r	natural coordinate
S	location of moving interface
s	natural coordinate
Ste	Stefan number
T	temperature
\underline{T}	temperature matrix
T_i	initial temperature
T_m	saturation temperature
t	time
\underline{U}	velocity matrix in x direction
$\underline{U}^{(s)}$	displacement interpolation matrix
u	velocity of fluid in x direction
\underline{V}	velocity matrix in y direction
v	velocity of fluid in y direction
v_n	normal velocity of moving interface
x	space variable
y	space variable

Greek Letters

α	thermal diffusivity
β	thermal expansion coefficient
Γ	boundary of domain
Δt	time step
E	moving boundary
θ	dimensionless temperature
λ	penalty constant
ρ	density
τ	tangential direction
Ω	time dependent domain
$\partial\Omega$	surface of time dependent domain
ω_j	weighting function
ν	viscosity

Superscript

*	dimensionless quantity
T	transpose
s	on boundary surface
(s)	on the moving surface
i	iteration i

Subscript

1	region 1
2	region 2
n	in the normal direction
mi	moving interface
x	in the x direction

Introduction

In recent years it has become increasingly important to understand precisely the physical phenomena that control the shape of the solid-liquid interface during solidification processes. A precise understanding can facilitate accurate control over the shape of the interface during various industrial processes in which materials are produced by solidification from melt. Control over the shape of the interface is especially important in semiconductor crystal growth from melt.

In the past, most studies dealing with phase change problems have concentrated on the conduction heat transfer mechanism [1,2,3]. However, in recent years, the study of fluid flow in the melt and the study of the effects of fluid flow on the solid-liquid interface morphology has acquired major importance [1,4-17]. Fluid flow due to natural convection occurs in a majority of solidification processes where parts of the melt are at a temperature higher than the phase transition temperature. This paper presents a new numerical method for the analysis of transient solidification processes in the presence of natural convection. It will be also shown that natural convection can have a large influence on the morphology of the solid-liquid interface, the solidification rate and the temperature distribution in the liquid and the solid.

Specific to heat transfer problems with phase transformation is the existence of an interface that separates between the solid and liquid phases. The location of the interface changes in time as a function of the thermal boundary conditions, in a way that is unknown prior to the solution of the problem. The displacement of this interface is responsible for the nonlinearity of the problem.

A general analysis of solidification processes is made difficult by the need to solve the nonlinear problem in a transient irregular domain with geometrical boundaries unknown prior to the solution of the problem. Numerous analytical methods have been developed in recent years for the solution of this problem. Many of the methods have been summarized in references [3,18,19]. Numerical methods using finite elements have been also reported in the past. The numerical techniques involving finite elements can be separated into two distinct groups based on the formulation of the problem. In the first group enthalpy is the dependent variable [20,21]. The second group deals with the energy equation written in terms of temperature as the dependent variable [22,23]. Many solutions of the heat transfer equation in the presence of phase transformation in which the temperature is the dependent variable involve the technique of moving elements or deforming elements. Moving or deforming elements are also commonly used in other types of problems with free interfaces, i.e., surface seepage [24].

Bonnerot and Janet [22] were the first to develop a method using deforming elements for phase transformation problems. They discretize the domain by means of isoparametric finite elements corresponding to a six-noded triangular prism in a space defined by the x,y Cartesian coordinates and t , the space variable. The free boundary is approximated by a polygon line whose vertices coincide with triangulation nodes. In this method the change of phase interface is tracked continuously in time while the elements deform continuously. Other studies using moving or deforming elements and tracking the change of phase interface have been reported in references [22,25-29].

The effects of natural convection on the solidification process has been discussed in several recent papers. Some of these studies using numerical

methods of solution will be described briefly. Kroeger and Ostrach [17], solved the freezing problem in the presence of natural convection for a two dimensional continuous slab casting problem. They used iterative finite difference and conformal transformation of the domain. Sparrow, Patankar and Ramahyani [6] have analyzed the melting of a solid in a cylindrical enclosure considering natural convection in the liquid. They applied the implicit finite difference scheme to the transformed domain in which the interface had a tractable shape. Yao and Chen [13] have developed a perturbation solution for the melting problem around a heated horizontal cylinder. The solution was limited to small Rayleigh numbers and small Stefan numbers. Ramachandran, Gupta and Jaluria [14,15] reported two papers on solidification including natural convection effects in the liquid. They use an Alternative Direction Implicit Technique with an Over-Relaxation Method. The moving boundary equation was solved using a Chebyshev approximation. Gadgil and Gobin [16] have analyzed the melting in a regular enclosure considering natural convection in the liquid region. They divided the process in a number of quasi-static steps and solved for the steady state natural convection flow in the liquid region.

The problem of phase transformation with fluid flow is complicated by the need to solve in the liquid domain the momentum equation as well as the energy equation. Furthermore, fluid flow boundary conditions must be imposed on a moving boundary. Recently we have developed a new finite element method for the analysis of solidification processes. The new method which belongs to the class of "front tracking" finite element methods has been described by us in references [26-29]. The method has been proven to be efficient for the analysis of transient solidification processes in irregular geometries with transient and spatially variable boundary conditions. This method is very well suited for the

solution of phase transformation problems with fluid flow and in this work we will present the use of the "front tracking" finite element method for the analysis of solidification processes in the presence of natural convection. The fluid flow in the liquid region will be analyzed using a finite element formulation of the momentum equation in terms of primitive variables (velocity and pressure), and using a "penalty" method to eliminate the pressure variable from the equations. Following a general description of the method a specific numerical example dealing with transient solidification in a 2-dimensional rectangular enclosure in the presence of transient natural convection will be solved.

Description of the Problem

Solidification in the presence of natural convection will be considered in the two time-dependent domains $\Omega_1(t)$ and $\Omega_2(t)$ in R^2 (Fig. 1) representing the solid and liquid phases. A constant domain D exists such that

$D = \Omega_1(t) \cup \Omega_2(t)$. The boundaries of the domains are $\partial\Omega_1(t) = \Gamma_1(t) \cup \epsilon(t)$ and $\partial\Omega_2(t) = \Gamma_2(t)$, where $\epsilon(t)$ is the moving change of phase interface common to $\Omega_1(t)$ and $\Omega_2(t)$. The outward normal unit vector at any point $P \in \partial\Omega_1(t)$ is n_1 and at any point $P \in \partial\Omega_2(t)$ is n_2 . We will also use the notation:

$$\begin{aligned}
 \Sigma_1 &= \{(P,t) : P \in \Gamma_1 \quad t > 0\} \\
 \Sigma_2 &= \{(P,t) : P \in \Gamma_2 \quad t > 0\} \\
 S &= \{(P,t) : P \in \epsilon(t) \quad t > 0\} \\
 R_1 &= \{(P,t) : P \in \Omega_1(t) \quad t > 0\} \\
 R_2 &= \{(P,t) : P \in \Omega_2(t) \quad t > 0\}
 \end{aligned} \tag{1}$$

The following physical assumptions are made in the formulation of the problem.

- (1) The physical properties of the solid and liquid are assumed to be constant except the density difference due to temperature variation in the liquid, which contributes to the buoyancy forces (Boussinesq approximation).
- (2) The flow developed in the liquid due to the thermal gradients is assumed to be laminar.
- (3) The liquid is assumed to be Newtonian with negligible viscous energy dissipation.

Kinematic no-slip condition on the wall as well as on the solid-liquid interface are imposed.

The governing equations are nondimensionalized by employing the following parameters and dimensionless variables.

$$\begin{array}{lll}
 x^* = x/L & u^* = uL/\alpha & Ste = c_p (T_i - T_m)/H_{sl} \\
 y^* = y/L & v^* = vL/\alpha & Ste^* = Ste k_1/k_2 \\
 t^* = t\alpha_2/L^2 & H = \ell/L & R_\alpha = \alpha_1/\alpha_2 \\
 \theta = (T - T_m)/(T_i - T_m) & Ra = g\beta (T_i - T_m)L^3/\nu\alpha_2 & R_k = k_1/k_2 \\
 & Pr = \nu/\alpha_2 & Pd^* = Pd/\rho\alpha_2L^2
 \end{array} \tag{2}$$

Our problem is to determine the variable position of the moving interface, the temperature distribution and velocity distribution from the following nondimensionalized equation and boundary conditions.

Continuity:

$$\frac{\partial u_i^*}{\partial x_i^*} = 0 \quad (3)$$

momentum:

$$\frac{\partial u_i^*}{\partial t^*} + u_j^* \frac{\partial \theta_2}{\partial x_j^*} = - \frac{\partial p_d^*}{\partial x_i^*} + Pr \frac{\partial}{\partial x_j^*} \left(\frac{\partial u_i^*}{\partial x_j^*} + \frac{\partial u_j^*}{\partial x_i^*} \right) - Pr Ra f_i \theta_2 \quad (4)$$

energy in liquid:

$$\frac{\partial \theta_2}{\partial t^*} + u_j^* \frac{\partial \theta_2}{\partial x_j^*} = \frac{\partial}{\partial x_i^*} \left(\frac{\partial \theta_2}{\partial x_i^*} \right) \quad (5)$$

energy in solid:

$$\frac{\partial \theta_1}{\partial t^*} = R_\alpha \frac{\partial \theta_2}{\partial x_i^*} \left(\frac{\partial \theta_2}{\partial x_i^*} \right) \quad (6)$$

energy balance on the moving interface:

$$\frac{\partial \theta_1}{\partial n^*} - R_k^{-1} \frac{\partial \theta_2}{\partial n^*} = Ste^{*-1} v_n^* \quad (7)$$

where v_n^* is the velocity of the interface in the direction n_1 , normal to the interface.

initial conditions:

$$\text{at } t^* = 0; \theta_1 = \theta_1^0 \text{ in } R_1 \quad (8)$$

$$\theta_2 = \theta_2^0 \text{ in } R_2$$

energy boundary condition:

$$a_1^* \nabla^* \theta_1 n_1^* + b_1^* \theta_1 = c_1^* \quad \text{on } \Sigma_1 \quad (9)$$

$$a_2^* \nabla^* \theta_2 n_2^* + b_2^* \theta_2 = c_2^* \quad \text{on } \Sigma_2 \quad (10)$$

$$\theta_1 = \theta_2 = 0 \quad \text{on } S \quad (11)$$

velocity boundary condition:

$$u^* = v^* = 0 \quad \text{on } \Sigma_2 \text{ and } S \quad (12)$$

Using the weight functions $\omega_1 \in H^1(R_1)$, $\omega_2 \in H^1(R_2)$, $\omega_3 \in H^1(R_3)$, and ω_4 (to be discussed later), the weak forms of Eqs. (3 to 6) are:

$$\int_{\Omega_2} \omega_1 \left[\frac{\partial u_i^*}{\partial t^*} + u_j^* \frac{\partial u_i^*}{\partial x_j^*} + \frac{\partial p_d^*}{\partial x_i^*} + \text{Pr} \frac{\partial}{\partial x_j^*} \left(\frac{\partial u_i^*}{\partial x_j^*} + \frac{\partial u_j^*}{\partial x_i^*} \right) + \text{Pr Ra} f_i \theta_2 \right] d\Omega = 0 \quad (13)$$

$$\int_{\Omega_2} \omega_2 \left[\frac{\partial \theta_2}{\partial t^*} + u_j^* \frac{\partial \theta_2}{\partial x_j^*} + \frac{\partial}{\partial x_j^*} \left(\frac{\partial \theta_2}{\partial x_j^*} \right) \right] d\Omega = 0 \quad (14)$$

$$\int_{\Omega_1} \omega_3 \left[\frac{\partial \theta_1}{\partial t^*} - \frac{\partial}{\partial x_j^*} \left(R_\alpha \frac{\partial \theta_1}{\partial x_j^*} \right) \right] d\Omega = 0 \quad (15)$$

$$\int_S \omega_4 \left[\text{Ste}^{*-1} v_n^* \right] ds = \int_S \omega_4 \left[\frac{\partial \theta_1}{\partial n^*} - R_k^{-1} \frac{\partial \theta_2}{\partial n^*} \right] ds \quad (16)$$

where Ω_i denotes the problem domain and S denotes phase interface. The divergence theorem is applied to reduce the order of differentiation in

Eqs. (13-15) and introduce boundary integral terms containing the heat flux and stress vector.

$$\int_{\Omega_2} \left[\omega_1 \left(\frac{\partial u_i^*}{\partial t^*} + u_j^* \frac{\partial u_i^*}{\partial x_j^*} + \text{Pr Ra } f_i \theta_2 \right) - P_d^* \frac{\partial \omega_1}{\partial x_i^*} \right. \\ \left. + \text{Pr} \frac{\partial \omega_1}{\partial x_j^*} \left(\frac{\partial u_i^*}{\partial x_j^*} + \frac{\partial u_j^*}{\partial x_i^*} \right) \right] d\Omega = \int_{\partial\Omega_2} \omega_1 t_i ds \quad (17)$$

$$\int_{\Omega_2} \left[\omega_2 \left(\frac{\partial \theta_2}{\partial t^*} + u_j^* \frac{\partial u_i^*}{\partial x_j^*} \right) + \frac{\partial \omega_2}{\partial x_j^*} \left(\frac{\partial \theta_2}{\partial x_j^*} \right) \right] d\Omega \\ = - \int_{\partial\Omega_2} \omega_2 q_2^s ds \quad (18)$$

$$\int_{\Omega_1} \left[\omega_3 \frac{\partial \theta_1}{\partial t^*} + R_\alpha \frac{\partial \omega_3}{\partial x_j^*} \left(\frac{\partial \theta_1}{\partial x_j^*} \right) \right] d\Omega = - \int_{\partial\Omega_1} \omega_3 q_1^s ds \quad (19)$$

where

$$t_i = \left[-P_d^* \delta_{ij} + \text{Pr} \frac{\partial}{\partial x_j^*} \left(\frac{\partial u_i^*}{\partial x_i^*} + \frac{\partial u_j^*}{\partial x_i^*} \right) \right] n_j^* \\ q_1^* = - \frac{\partial \theta_1}{\partial x_i^*} n_{1i}^*$$

and

$$q_2^* = - \frac{\partial \theta_2}{\partial x_i} n_{2i}^*$$

Probably our most significant contribution in this paper deals with the finite element formulation of equation (16). The solution of equation (16) together with that of equations (17) to (19) can give only the magnitude of the displacement of the solid-liquid interface in time in a direction normal to the interface. The direction of the normal is not known however. Of course, tracking in time continuously the interface could provide at each instant the direction of the normal. Nevertheless, the direction has to be evaluated independently. The difficulties associated with the accurate determination of the normal to a surface (a derivative) in a finite element formulation of the problem are significant. To overcome the difficulties associated with the need to determine the direction of the normal, a new method was developed by which equation (16) is decomposed into two different components in the x and y direction. The procedure is based on a special physical argument not employed in the past for phase transformation problems.

The solid-liquid interface can be described at each point by the normal vector to the surface, n and by the surface s . The derivatives in the n and s direction can be correlated to derivatives in the x and y direction through the translation Jacobian, J based on the angle α , which is the angle between the direction of the normal to the interface and the x direction. The correlation can be expressed by

$$\begin{bmatrix} \frac{\partial}{\partial n} \\ \frac{\partial}{\partial s} \end{bmatrix} = \begin{bmatrix} \frac{\partial x}{\partial n} & \frac{\partial y}{\partial n} \\ \frac{\partial x}{\partial s} & \frac{\partial y}{\partial s} \end{bmatrix} \begin{bmatrix} \frac{\partial}{\partial x} \\ \frac{\partial}{\partial y} \end{bmatrix} = \begin{bmatrix} \cos\alpha & \sin\alpha \\ -\sin\alpha & \cos\alpha \end{bmatrix} \begin{bmatrix} \frac{\partial}{\partial x} \\ \frac{\partial}{\partial y} \end{bmatrix} \quad (20)$$

Using expression (20), equation (7) can be written as,

$$\text{Ste}^{*-1} \cdot v_n^* = \left[\left(\frac{\partial \theta_1}{\partial x} \cos \alpha + \frac{\partial \theta_1}{\partial y} \sin \alpha \right) - R_k^{-1} \left(\frac{\partial \theta_2}{\partial x} \cos \alpha + \frac{\partial \theta_2}{\partial y} \sin \alpha \right) \right] \quad (21)$$

since the velocity of any point on the change of phase interface θ_n^* is a vectorial quantity it can be expressed by

$$v_n^* \cdot \bar{n} = v_{nx}^* \cdot \bar{i} + v_{ny}^* \cdot \bar{j} \quad (22)$$

The component of velocity in the x direction can be expressed in terms of the velocity in the normal direction,

$$v_{nx}^* = v_n^* \cdot \bar{n} \cdot \bar{i} = v_n^* \cdot \cos \alpha \quad (23)$$

multiplying equation (21) by, $\cos \alpha$, and reorganizing terms yields

$$\text{Ste}^{*-1} \cdot v_{nx}^* = \left[\left(\frac{\partial \theta_1}{\partial x} - R_k^{-1} \frac{\partial \theta_2}{\partial x} \right) \cos \alpha + \left(\frac{\partial \theta_1}{\partial y} - R_k^{-1} \frac{\partial \theta_2}{\partial y} \right) \sin \alpha \right] \cos \alpha \quad (24)$$

In regular solutions to heat transfer problems with phase transformation only equation (7), the energy balance in the direction normal to the interface is used. The energy balance in the direction tangential is never considered. This balance contains, however, significant information which will be used in our analysis. The statement for the energy balance in the tangential direction is

$$\frac{\partial \theta_1}{\partial s} - R_k^{-1} \frac{\partial \theta_2}{\partial s} = 0 \quad (25)$$

Equation (25) can also be viewed as a statement that the solid liquid interface is isothermal. Using equation (20), equation (25) can be written in terms of derivatives in the x and y direction

$$\left(-\frac{\partial \theta_1}{\partial x^*} \sin \alpha + \frac{\partial \theta_1}{\partial y^*} \cos \alpha\right) - R_k^{-1} \left(-\frac{\partial \theta_2}{\partial x^*} \sin \alpha + \frac{\partial \theta_2}{\partial y^*} \cos \alpha\right) = 0 \quad (26)$$

when equation (26) is organized and introduced in the terms multiplied by $\sin \alpha$ in equation (24) the following equation is obtained

$$\text{Ste}^{-1} v_{nx}^* = \frac{\partial \theta_1}{\partial x^*} - R_k^{-1} \frac{\partial \theta_2}{\partial x^*} \quad (27a)$$

A similar decomposition in the y direction yields

$$\text{Ste}^{-1} v_{ny}^* = \frac{\partial \theta_1}{\partial y^*} - R_k^{-1} \frac{\partial \theta_2}{\partial y^*} \quad (27b)$$

where v_{nx}^* is the nondimensional velocity of each point P on S, the interface, in the x direction and v_{ny}^* is the nondimensional velocity of each point P on the interface in the y direction. Since by definition v_{nx}^* and v_{ny}^* are the velocities of each point P on S in the x and y direction respectively, more convenient notations are used:

$$v_{nx}^* = \left(\frac{\partial S}{\partial t^*}\right)_x \quad v_{ny}^* = \left(\frac{\partial S}{\partial t^*}\right)_y \quad (28)$$

Equation (28) indicates that the velocity of the interface in the x or y direction is identical to the rate of displacement of each point P on S in the x or y direction.

A simplified example will be used to introduce the finite element formulation of Eqs. (27) and (28). Consider the simplified situation illustrated in Fig. 2, where the domains Ω_1 and Ω_2 are each represented by a four-node isoparametric element and the moving interface $S(t)$ is the common line of these domains. The displacement of the interface could be expressed in terms of the

displacement of the nodes on the moving surface by using the displacement interpolation matrix on the moving interface $\underline{H}^{(s)}$ such that

$$(dS)_x = \underline{H}^{(s)} \underline{dx}_i^* \text{ and } (dS)_y = \underline{H}^{(s)} \underline{dy}_i^* \quad (29)$$

where $\underline{H}^{(s)} = [1/2 (1 + r), 1/2 (1 - r)]$, x_i^* and y_i^* are the x and y dimensionless coordinates of the nodal points, and $(dS)_x$ and $(dS)_y$ are the dimensionless displacements in the x and y directions respectively of all the points on S. Since S is a continuous function, the velocity of the moving interface at each point P on S can also be expressed in terms of the velocity at the nodes and the interpolation function $\underline{H}^{(s)}$ such that

$$\left(\frac{\partial S}{\partial t^*} \right)_x = \underline{H}^{(s)} \frac{dx_i^*}{dt^*} \quad \cdot \quad \left(\frac{\partial S}{\partial t^*} \right)_y = \underline{H}^{(s)} \frac{dy_i^*}{dt^*} \quad (30)$$

The displacement of each point P on S can be expressed in terms of the displacement of that point in the x and y directions in a general formulation

$$\begin{bmatrix} dS \end{bmatrix} = \begin{bmatrix} (dS)_x \\ (dS)_y \end{bmatrix} = \begin{bmatrix} \underline{H}^{(s)} \underline{dx}_i^* \\ \underline{H}^{(s)} \underline{dy}_i^* \end{bmatrix} \quad (31)$$

To simplify the notation, introduce a new matrix,

$$\begin{bmatrix} dS \end{bmatrix} = \underline{U}^{(s)} \begin{bmatrix} dS \end{bmatrix} \quad (32)$$

where $\underline{U}^{(s)}$ is the combination of interpolation function in Eq. (30) which for the specific situation discussed in this example becomes

$$\underline{u}(s) = \begin{bmatrix} \frac{1}{2}(1+r) & 0 & \frac{1}{2}(1-r) & 0 \\ 0 & \frac{1}{2}(1+r) & 0 & \frac{1}{2}(1-r) \end{bmatrix} \quad (33)$$

and \underline{dS} is the dimensionless nodal displacement vector defined by

$$\underline{dS} = \begin{bmatrix} dx_1^* \\ dy_1^* \\ dx_2^* \\ dy_2^* \end{bmatrix} \quad (34)$$

where the subscripts 1 and 2 stand for the two nodes on the interface shown in Fig. 2. From Eqs. (29) to (34) the velocity in the x and y direction of the interface can be expressed in terms of the interpolation function $\underline{u}(s)$ such that

$$\begin{bmatrix} v_{nx}^* \\ v_{ny}^* \end{bmatrix} = \begin{bmatrix} \left(\frac{\partial S}{\partial t^*} \right)_x \\ \left(\frac{\partial S}{\partial t^*} \right)_y \end{bmatrix} = \underline{u}(s) \cdot \frac{dS}{dt^*} \quad (35)$$

Equation (27) can be introduced now in the finite element formulation equation (16) to yield

$$\int_s \omega_4 \begin{bmatrix} Ste^{-1} v_{nx}^* \\ Ste^{-1} v_{ny}^* \end{bmatrix} dS = \int_s \omega_4 \begin{bmatrix} \frac{\partial \theta_1}{\partial x} - R_k^{-1} \frac{\partial \theta_2}{\partial x} \\ \frac{\partial \theta_2}{\partial y} - R_k^{-1} \frac{\partial \theta_2}{\partial y} \end{bmatrix} \underline{dS} \quad (36)$$

Following the Galerkin method [31] we seek a weighting function ω_4 in the same space as the interface velocity function. The basic interpolation function

\underline{U}_s can be used to define such a space. Accordingly, using Eq. (36), a weak formulation can be obtained for (7) and (16). The solution of the resulting equation will provide the displacement of each node on the solid-liquid interface in the x and y direction independently. For the simplified example in Fig. 2, Eq. (36) becomes

$$\int_{-1}^1 \underline{U}^{(s)T} \left[\underline{B}_1^{(s)} \cdot \underline{T}_1 - R_k^{-1} \cdot \underline{B}_2^{(s)} \underline{T}_2 \right] \det \underline{J}^{(s)} dS = \int_{-1}^1 Ste^{*-1} \underline{U}^{(s)T} dS. \quad (37)$$

$$\underline{U}^{(s)} \frac{dS}{dt} \det \underline{J}^{(s)} dS$$

Here $\underline{B}_1^{(s)}$ and $\underline{B}_2^{(s)}$ are the known dimensionless temperature gradient matrices on the moving interface in domains 1 and 2 respectively and $\underline{U}^{(s)}$ is the surface interpolation matrix defined in Eq. (33), \underline{T}_1 and \underline{T}_2 are the dimensionless temperature vectors. The determinant of $\underline{J}^{(s)}$ on the moving interface shown in Fig. 2 is given by

$$\det \underline{J}^{(s)} = \frac{1}{2} \left((x_1 - x_2)^2 + (y_1 - y_2)^2 \right)^{1/2} \quad (38)$$

The $\underline{B}_1^{(s)}$ matrix is given as

$$\underline{B}_1^{(s)} = \frac{1}{4} \frac{J^{-1}}{s=1} \begin{bmatrix} 2 & -2 & 0 & 0 \\ (1+r) & (1-r) & -(1-r) & -(1+r) \end{bmatrix} \quad (39)$$

The $\underline{B}_1^{(s)}$ matrix is typical of all common finite element formulations. It is evident that if the dimensionless nodal temperature vectors \underline{T}_1 and \underline{T}_2 are known at each instance in time, the solution of Eq. (37) yields the displacement of the interface in time.

It is important to note that to solve the finite element formulation of Eq. (36) the elements in domains $\Omega_1(t)$ and $\Omega_2(t)$ must satisfy the compatibility requirement at the moving interface. With this restriction in mind, the general finite element formulation for equation (6) becomes:

$$\underline{A}_1 \underline{I}_1 - \underline{A}_2 \underline{I}_2 = \underline{L}_{ph} \frac{dS}{dt} \quad (40)$$

where, \underline{I}_1 and \underline{I}_2 are the dimensionless temperature vectors and,

$$\underline{A}_1 = \sum_m \int_{\Sigma(t)} \underline{U}^{(m)}(s)^T \underline{B}_1^{(m)}(s) ds$$

$$\underline{A}_2 = \sum_m \int_{\Sigma(t)} R_k^{-1} \underline{U}^{(m)}(s)^T \underline{B}_2^{(m)}(s) ds$$

$$\underline{L}_{ph} = \sum_m \int_{\Sigma(t)} Ste^{*-1} \underline{U}^{(m)}(s)^T \underline{U}^{(m)}(s) ds$$

The solution of Eqs. (39,40) provides the displacement in the x and y direction of nodes on the solid liquid interface for a known temperature distribution in the solid and liquid domains. To determine the temperature distribution in the solid and liquid domains Eqs. (17) to (19) must be solved together with Eq. (40).

Equation (19) representing the energy balance in the solid region does not present any significant difficulties. Dividing the solid domain and the attendant temperatures into isoparametric element with a variable number of nodes yields for Eq. (19) a standard finite element formulation [30,31].

$$\underline{M}_1 \underline{T}_1 + \underline{K}_1 \underline{T}_1 = \underline{Q}_1 \quad (41)$$

where

$$\underline{M}_1 = \sum_m \int_{-1}^1 \int_{-1}^1 \underline{H}^T \underline{H} \det \underline{J} \, dr ds$$

$$\underline{K}_1 = \sum_m \int_{-1}^1 \int_{-1}^1 k \underline{B}^T \underline{B} \det \underline{J} \, dr ds$$

$$\underline{Q}_1 = \int_{\partial \Omega_j} \underline{H}^S \underline{q}^S \, ds$$

and the summation is over all element in the solid domain.

Equations (2) (17) and (18) are more difficult to solve.

The basic approach in the solution of the momentum equation has been to employ finite element approximation to the governing partial differential equations expressed in terms of the stream function and vorticity [32,33]. The major advantage offered by this approach is the identical satisfaction of the continuity equation, or incompressibility constraint, through the introduction of the stream function or vector potential and the elimination of the pressure as an explicit variable when the vorticity is considered as a dependent variable. However, this method suffers from the disadvantage of the need to improve boundary conditions on the vorticity. Since we deal in this problem with a moving boundary and since velocity boundary conditions must be imposed on this boundary, a formulation using the primitive variables, velocity and pressure, was used here. The fluid mechanics problem was solved using a "penalty" method. In this method the compressibility condition is viewed as a constraint on the velocity field that satisfies the momentum equations. The

penalty method was presented first by Courant Friedrichs and Levy [34] was used first in finite elements by Babuska [35] and in fluid flow by Zienkiewicz [36].

As the popularity of the penalty finite element method grew, a large number of solutions have appeared in the literature [37-41]. The penalty method is explained in several textbooks [23,33,34] and we will not dwell on the details of the method except as it is applied to this specific problem.

The continuity equation, Eq. (2), in its weighted form is:

$$\int_{\Omega_2} V_i \frac{\partial u_j^*}{\partial x_j} d\Omega = 0 \quad (42)$$

where V_i is an appropriate weighting function. The penalty method applied to the momentum equation, Eq. (17), with the continuity equation, Eq. (42) requires that the pressure be expressed by [40],

$$P_d^* = -\lambda \frac{\partial u_j^*}{\partial x_j} \quad (43)$$

Using equation (43) in (17) satisfies implicitly equation (42) and also eliminates the pressure, P_d^* , as an explicit variable in Eq. (17).

Then Eq. (17) becomes:

$$\int_{\Omega_2} \left[\omega_1 \left(\frac{\partial u_i^*}{\partial t} + u_j^* \frac{\partial u_i^*}{\partial x_j} + \text{Pr Ra } f_i \theta_2 \right) + \lambda \frac{\partial \omega_1}{\partial x_i} \frac{\partial u_j^*}{\partial x_j} \right. \\ \left. + \text{Pr} \frac{\partial \omega_1}{\partial x_j} \left(\frac{\partial u_i^*}{\partial x_j} + \frac{\partial u_j^*}{\partial x_i} \right) \right] d\Omega = \int_{\partial\Omega_2} \omega_1 t_i ds \quad (44)$$

Solution Methodologies

Equation (44) is obviously nonlinear. To facilitate the solution several simplifications were introduced in the iteration procedure. These can be described as modified Newton-Raphson iteration procedures. To remove the nonlinearity associated with the velocity u_j^* in the second term in equation (42), during each iteration the value of u_j^* , was taken to be that in the previous iteration, ${}^i u_j^*$. Following a standard finite element procedure, in which the geometric domain and the attendant velocities and temperatures are divided into isoparametric elements with a variable number of nodes; equations (44), (18) (19) and (38) take the general form:

$$\begin{bmatrix} \underline{M}_2 & 0 & 0 \\ 0 & \underline{M}_2 & 0 \\ 0 & 0 & -\underline{M}_2 \end{bmatrix} \begin{bmatrix} \dot{\underline{U}} \\ \dot{\underline{V}} \\ \dot{\underline{T}}_2 \end{bmatrix} + \begin{bmatrix} \underline{C}_{11} + \underline{C}_{22} & 0 & 0 \\ 0 & \underline{C}_{11} + \underline{C}_{22} & 0 \\ 0 & 0 & \underline{C}_{11} + \underline{C}_{22} \end{bmatrix} \begin{bmatrix} \underline{U} \\ \underline{V} \\ \underline{T}_2 \end{bmatrix} \quad (45)$$

$$+ \text{Pr Ra} \begin{bmatrix} 0 & 0 & f_1 \underline{M}_2 \\ 0 & 0 & f_2 \underline{M}_2 \\ 0 & 0 & 0 \end{bmatrix} \begin{bmatrix} \underline{U} \\ \underline{V} \\ \underline{T}_2 \end{bmatrix} + \text{Pr} \begin{bmatrix} 2\underline{K}_{11} + \underline{K}_{22} & \underline{K}_{12} & 0 \\ \underline{K}_{12}^T & \underline{K}_{11} + 2\underline{K}_{22} & 0 \\ 0 & 0 & \text{Pr}^{-1} \underline{K}_2 \end{bmatrix} \begin{bmatrix} \underline{U} \\ \underline{V} \\ \underline{T}_2 \end{bmatrix}$$

$$+ \lambda \begin{bmatrix} \underline{L}_{11} & \underline{L}_{12} & 0 \\ \underline{L}_{12}^T & \underline{L}_{22} & 0 \\ 0 & 0 & 0 \end{bmatrix} \begin{bmatrix} \underline{U} \\ \underline{V} \\ \underline{T}_2 \end{bmatrix} = \begin{bmatrix} \underline{R}_1 \\ \underline{R}_2 \\ \underline{Q}_2 \end{bmatrix}$$

$$\underline{M}_1 \dot{\underline{I}}_1 + \underline{K}_1 \underline{I}_1 = Q_1 \quad (46)$$

$$\underline{A}_1 \underline{I}_1 - \underline{A}_2 \underline{I}_2 = L_{ph} \frac{dS}{dt} \quad (47)$$

where

$$\underline{M}_1 = \sum_{m_1} \int_{\Omega_1^{(m)}} \underline{H}^{(m)T} \underline{H}^{(m)} d\Omega$$

$$\underline{C}_{-i i} = \sum_{m_i} \int_{\Omega_1^{(m)}} i_{\underline{u}_i} \underline{H}^{(m)T} \underline{B}_i^{(m)} d\Omega \quad (48)$$

$$\underline{K}_{-i j} = \sum_{m_2} \int_{\Omega_2^{(m)}} \underline{B}_i^{(m)T} \underline{B}_j^{(m)} d\Omega$$

$$\underline{L}_{ij} = \sum_{m_2} \int_{\Omega_2^{(m)}} \underline{B}_i^{(m)T} \underline{B}_j^{(m)} d\Omega \quad (49)$$

$$\underline{R}_i = \sum_{n_2} \int_{\Omega_2^{(m)}} t_i H^s^{(m)} ds \quad (50)$$

$$\underline{K}_{ij} = \sum_{m_1} \int_{\Omega_1^{(m)}} \underline{B}_i^{(m)T} \underline{B}_j^{(m)} d\Omega \quad (51)$$

$$\underline{Q}_i = \sum_{n_1} \int_{\Omega_1^{(m)}} -q_i^s H^s^{(m)} ds \quad (52)$$

A modified implicit integration scheme is used for Eqs. (45) and (46) and an explicit scheme is used for Eq. (47):

$$\frac{1}{\Delta t} \begin{bmatrix} M_2^{t^*+\Delta t^*} & 0 & 0 \\ 0 & M_2^{t^*+\Delta t^*} & 0 \\ 0 & 0 & M_2^{t^*+\Delta t^*} \end{bmatrix} \begin{bmatrix} \underline{U}^{t^*+\Delta t^*} - \underline{U}^t \\ \underline{V}^{t^*+\Delta t^*} - \underline{V}^t \\ \underline{I}_2^{t^*+\Delta t^*} - \underline{I}_2^t \end{bmatrix} + \begin{bmatrix} C_{-11}^{t^*+\Delta t^*} + C_{-22}^{t^*+\Delta t^*} & 0 & 0 \\ 0 & C_{-11}^{t^*+\Delta t^*} + C_{-22}^{t^*+\Delta t^*} & 0 \\ 0 & 0 & C_{-11}^{t^*+\Delta t^*} + C_{-22}^{t^*+\Delta t^*} \end{bmatrix}$$

$$\begin{bmatrix} \underline{U}^{t^*+\Delta t^*} \\ \underline{V}^{t^*+\Delta t^*} \\ \underline{I}_2^{t^*+\Delta t^*} \end{bmatrix} + \text{Pr Ra} \begin{bmatrix} 0 & 0 & f_{1-2} M_2^{t^*+\Delta t^*} \\ 0 & 0 & f_{2-2} M_2^{t^*+\Delta t^*} \\ 0 & 0 & 0 \end{bmatrix} \begin{bmatrix} \underline{U}^{t^*+\Delta t^*} \\ \underline{V}^{t^*+\Delta t^*} \\ \underline{I}_2^{t^*+\Delta t^*} \end{bmatrix} + \quad (53)$$

$$+ \text{Pr} \begin{bmatrix} 2K_{-11}^{t^*+\Delta t^*} + K_{-22}^{t^*+\Delta t^*} & K_{-12}^{t^*+\Delta t^*} & 0 \\ K_{-12}^{t^*+\Delta t^*T} & K_{-11}^{t^*+\Delta t^*} + 2K_{-22}^{t^*+\Delta t^*} & 0 \\ 0 & 0 & \text{Pr}^{-1} K_{-2}^{t^*+\Delta t^*} \end{bmatrix} \begin{bmatrix} \underline{U}^{t^*+\Delta t^*} \\ \underline{V}^{t^*+\Delta t^*} \\ \underline{I}_2^{t^*+\Delta t^*} \end{bmatrix}$$

$$+ \lambda \begin{bmatrix} L_{-11}^{t^*+\Delta t^*} & L_{-12}^{t^*+\Delta t^*} & 0 \\ L_{-12}^{t^*+\Delta t^*T} & L_{-22}^{t^*+\Delta t^*} & 0 \\ 0 & 0 & 0 \end{bmatrix} \begin{bmatrix} \underline{U}^{t^*+\Delta t^*} \\ \underline{V}^{t^*+\Delta t^*} \\ \underline{I}_2^{t^*+\Delta t^*} \end{bmatrix} = \begin{bmatrix} R_1^{t^*+\Delta t^*} \\ R_2^{t^*+\Delta t^*} \\ Q_2^{t^*+\Delta t^*} \end{bmatrix}$$

$$\frac{1}{\Delta t^*} M_1^{t^*+\Delta t^*} (\underline{I}_1^{t^*+\Delta t^*} - \underline{I}_1^{t^*}) + \frac{K_1^{t^*+\Delta t^*}}{\underline{I}_1^{t^*+\Delta t^*}} \underline{I}_1^{t^*+\Delta t^*} = \underline{Q}_1^{t^*+\Delta t^*} \quad (54)$$

$$\frac{A_1^{t^*+\Delta t^*}}{\underline{I}_1^{t^*+\Delta t^*}} \underline{I}_1^{t^*+\Delta t^*} - \frac{A_2^{t^*+\Delta t^*}}{\underline{I}_2^{t^*+\Delta t^*}} \underline{I}_2^{t^*+\Delta t^*} = \frac{1}{\Delta t^*} \underline{L}_{ph}^{t^*+\Delta t^*} (\underline{S}^{t^*+\Delta t^*} - \underline{S}^t) \quad (55)$$

Notice that in equation (45) the velocity vector is taken from the previous iteration. In equation (53) the velocity and temperature are coupled. Because of the convection term \underline{C}_{ij} the system of equations is not symmetric. To avoid this situation further modifications were introduced in equation (53).

The temperature and velocities are coupled only by the buoyancy term, the third term. If the temperature in the third term, $\underline{I}_2^{t^*+\Delta t^*}$ is replaced by its value during the previous iteration, $\underline{I}_2^{t^*}$ the velocities and temperature can be decoupled. Variables, $\underline{u}^{t^*+\Delta t^*}$, $\underline{v}^{t^*+\Delta t^*}$ and $\underline{I}^{t^*+\Delta t^*}$ in the convection term, the third term, were therefore replaced by their value during the previous iteration, \underline{u}^{t^*} , \underline{v}^{t^*} , and \underline{I}^{t^*} . Now the modified equations are given by:

$$\begin{aligned}
& \frac{1}{\Delta t^*} \begin{bmatrix} i+1_{M_2} t^{**+\Delta t^*} & 0 \\ 0 & i+1_{M_2} t^{**+\Delta t^*} \end{bmatrix} \cdot \begin{bmatrix} i+1_{\underline{U}} t^{**+\Delta t^*} - \underline{U}^t \\ i+1_{\underline{V}} t^{**+\Delta t^*} - \underline{V}^t \end{bmatrix} \\
& + \begin{bmatrix} i+1_{\underline{C}_{11}} t^{**+\Delta t^*} + i+1_{\underline{C}_{22}} t^{**+\Delta t^*} & 0 \\ 0 & i+1_{\underline{C}_{11}} t^{**+\Delta t^*} + i+1_{\underline{C}_{22}} t^{**+\Delta t^*} \end{bmatrix} \cdot \begin{bmatrix} i+1_{\underline{U}} t^{**+\Delta t^*} \\ i+1_{\underline{V}} t^{**+\Delta t^*} \end{bmatrix} \\
& + Pr Ra \begin{bmatrix} f_{1 \underline{M}_2}^{i+1} t^{**+\Delta t^*} & i_{\underline{T}_2} t^{**+\Delta t^*} \\ f_{1 \underline{M}_2}^{i+1} t^{**+\Delta t^*} & i_{\underline{T}_2} t^{**+\Delta t^*} \end{bmatrix} + \\
& + Pr \begin{bmatrix} i+1_{\underline{K}_{11}} t^{**+\Delta t^*} + i+1_{\underline{K}_{22}} t^{**+\Delta t^*} & i+1_{\underline{K}_{12}} t^{**+\Delta t^*} \\ i+1_{\underline{K}_{12}} (t^{**+\Delta t^*}) T & i+1_{\underline{K}_{11}} t^{**+\Delta t^*} + 2 i+1_{\underline{K}_{22}} t^{**+\Delta t^*} \end{bmatrix} \cdot \\
& \cdot \begin{bmatrix} i+1_{\underline{U}} t^{**+\Delta t^*} \\ i+1_{\underline{V}} t^{**+\Delta t^*} \end{bmatrix} + \\
& + \lambda \begin{bmatrix} i+1_{\underline{L}_{11}} t^{**+\Delta t^*} & i+1_{\underline{L}_{12}} t^{**+\Delta t^*} & i+1_{\underline{U}} t^{**+\Delta t^*} \\ i+1_{\underline{L}_{12}} t^{**+\Delta t^*} T & i+1_{\underline{L}_{22}} t^{**+\Delta t^*} & i+1_{\underline{V}} t^{**+\Delta t^*} \end{bmatrix} = \begin{bmatrix} i+1_{\underline{R}_1} t^{**+\Delta t^*} \\ i+1_{\underline{R}_2} t^{**+\Delta t^*} \end{bmatrix}
\end{aligned} \tag{56}$$

$$\frac{1}{\Delta t} \text{}^{i+1}_M 2t^{*+\Delta t*} \left(\text{}^{i+1}_I 2t^{*+\Delta t*} - \text{}^i_I 2t \right) + \left(\text{}^{i+1}_C 2t^{*+\Delta t*} + \text{}^{i+1}_C 2t^{*+\Delta t*} \right) \text{}^{i+1}_I 2t^{*+\Delta t*} \quad (57)$$

$$+ \text{}^{i+1}_K 2t^{*+\Delta t*} \text{}^{i+1}_I 2t^{*+\Delta t*} = \text{}^{i+1}_Q 2t^{*+\Delta t*}$$

Since the second and third terms of Eq. (56) are known they can be moved to the right hand side of the equation and treated as source terms. The second term of Eq. (57) is also known and can be moved to the right hand side and treated as a source term. This makes Eqs. (56) and (57) decoupled and all coefficient matrices become symmetric.

Computer Logic

The numerical scheme described above is not self-starting and the first step of the interface has to be calculated by using the Stefan solution for a semi-infinite medium. The consequent instability in the few steps following initiation of phase transformation is also typical of many other computer codes and decays rapidly.

The domain D is divided initially by a mesh generator into a predetermined number of elements. For the numerical experimentation described later in this work it was assumed that the phase transformation occurs from the outer surface of the domain to its interior, although more general situations can be handled as well. Nodes are initially generated, which coincide with the initial position of the change of phase interface. The nodes are set at predetermined equal spacing and are followed in time. A special procedure was developed to facilitate mesh generation at each time step and to track in time the nodes on the change of phase interface. Here one of the general nodal coordinate values of the interface is kept constant at every time step. For example, if the interface moves in the general x direction, the location of the moving nodes is

defined at each time step for a constant y coordinate value. At every time step we do not track the position of the old node but rather calculate from the displacement vector, dS the location of a new node on the interface at the constant y coordinate value. The new mesh is then generated according to the location of these nodes. The only constraint in meshing is that of element compatibility between the solid and liquid regions. The program which employs this mesh generation procedure is designed to limit only the maximum number of elements of Ω_1 and Ω_2 , and to have a fine mesh adjacent to walls and the interface. Therefore the number of elements in Ω_1 and Ω_2 can vary but cannot exceed a prescribed maximum number.

For each time step the fluid flow velocities were calculated first from equation (56). Then equation (57) was solved to determine the temperature distribution. Equations (56) and (57) were continuously iterated on until the velocity field and temperature field converged to an invariable value. It should be emphasized here that the matrices L_{ij} associated with the penalty parameter λ were integrated using a reduced Gauss integration order, a standard procedure with the penalty formulation.

Equation (54) was solved to obtain the temperature distribution in the solid phase. Equation (55) was then solved to obtain the displacement of the moving nodes on the change of phase interface. The whole domain was remeshed according to the new location of the nodes and the meshing procedure and the solution was marched forward in time.

Numerical Experiments

Numerical experiments were performed for solidification in a rectangular enclosure. The material to be solidified has been taken to be aluminum and its thermal properties are given in Table 1. A range of nondimensional parameters were tested. They are given in Table 2. Convective boundary conditions were assumed on one of the vertical walls of the rectangular enclosure of the form

$$\left. \frac{\partial \theta}{\partial n} \right|_{\text{wall}} = \text{Bi} (\theta_{\infty} - \theta_{\text{wall}})$$

while adiabatic boundary conditions were imposed on the other walls.

The maximum number of elements of each phase is 644. Calculations have been performed for different Rayleigh number, Ra , between 10^2 to 10^6 , for different aspect ratios of the rectangular enclosure, H , and environment temperature, θ_{∞} to study the natural convection effect on solidification process for the various situations. Between 50 to 70 time steps have been performed for each problem using the CDC 7600 in Lawrence Berkeley Laboratory. A typical running time was 2500 CPU seconds for 70 time steps. The large amount of CPU time has limited the calculation of higher Rayleigh numbers and further time steps. For example for $Ra = 10^6$, it took 500 CPU seconds for 5 time steps. The penalty constant plays a key role in assuring the convergence of the solution. If the penalty constant is too big or small, the solution could not converge or would need tremendous numbers of iterations at each step. A penalty constant of 10^8 was used for all Rayleigh numbers. This has proven to be sufficient to this application in this numerical experiment as well as in several previous investigations [41,43].

Typical vector plots of the velocity field and of the position of the change of phase interface for different times are shown in Figs. (3) (4) and

(5). These results were obtained for solidification in a rectangular domain $H = 1.0$, for an initial temperature higher by 200°C than the phase transition temperature, $\theta_\infty = -3$, and a Rayleigh number of $Ra = 10^5$. In the early stage of the solidification process (Fig. 3) the flow near the interface is almost parallel to the interface and downward. As time progresses the maximum velocity becomes much larger and the center of the flow cell moves farther and farther from the interface and from the bottom wall. The change of phase interface is evidently effected by the natural convection. The solidification process is much faster at the bottom of the enclosure. This is evidently caused by the fluid flow and the temperature distribution in the liquid region. The temperature distribution in the liquid domain, for the situation described by Figs. (3), (4) and (5) can be seen in Figs. (6), (7) and (8). It is seen that in an early stage of the solidification process the isothermal lines are almost parallel to the interface. Consequently the interface is planar. At a later stage, however, the fluid becomes stratified, (see Fig. 8), with a packet of hot fluid in the upper right hand side corner of the enclosure. This causes a decrease in the solidification rate in the upper side of the enclosure when compared to the lower side and the departure of the interface from a planar shape. The results presented above illustrate the need to incorporate fluid mechanics to accurately predict the solid-liquid interface morphology. Figure (9) which shows the movement of the solid-liquid interface in time, from left to right, illustrates the effect of the Rayleigh number on the interface morphology. It is seen that the higher the Rayleigh number the more will the interface depart from a planar shape.

Conclusions

A new numerical technique using finite elements has been developed for the study of heat transfer problems with phase transformation in the presence of natural convection. Specific to this method is the use of the energy equation on the solid-liquid interface to determine the displacement of the interface in time. This is done by finding separately the displacement of individual nodes on the interface in the x and y direction. The fluid flow equations in the liquid region were solved using a "penalty" method.

The new method developed in this work can cope with transient solidification processes in the presence of transient natural convection with arbitrary irregular and transient change of phase interface morphologies. The method has been tested successfully with solidification in two dimensional geometries. The results of our numerical experiments indicate that for Rayleigh numbers of the order of 10^4 to 10^5 , the solid-liquid interface morphology is strongly affected by the natural convection fluid flow. The new numerical method as well as the results of our numerical experiments are of importance for the controlled production of materials by solidification from melt.

Acknowledgement

This work was supported by the Director, Office of Energy Research, Office of Basic Energy Sciences, Materials Sciences Division of the U.S. Department of Energy under Contract No. DE-AC03-76SF00098.

The expert typing of Ms. L. Donahue is gratefully acknowledged.

References

1. Flemings, M.C., "Solidification Processing," McGraw-Hill, N.Y., 1979.
2. Rubinsky, B. and Shitzer, A., "Analysis of a Stefan-Like Problem in a Biological Tissue Around a Cryosurgical Probe," ASME J. Heat Trans., Vol. 98, No. 3, 1976, pp. 514-519.
3. Lunardini, V.J., "Heat Transfer in Cold Climates," Van Nostrand, N.Y., 1981.
4. Cole, G.S. and Bolling, G.F., "The Importance of Natural Convection in Casting," Trans. TMS-AIME, Vol. 233, 1965, pp. 1568,1572.
5. Szekely, J. and Stanek, V., "Natural Convection Transients and Their Effects of Unidirectional Solidification," Metall. Trans., Vol. 1, 1970, pp. 2243-2251.
6. Sparrow, E.M. Patankar, S.V., and Ramadhyani, S., "Analysis of Melting In the Presence of Natural Convection in the Melt Region," ASME J. Heat Trans., Vol. 99, 1977, pp. 520-526.
7. Seki, N., Fukusako, S., and Sugawara, M., "A Criterion of Onset of Free Convection in a Horizontal Melted Water Layer with a Free Surface," ASME, J. Heat Trans., Vol. 99, 1977, pp. 92-98.
8. Lame, G. and Claperyon, B.P., Ann. Chem. Phys., Vol. 47, 1831, pp. 250-256.
9. Vanier, C.R. and Tien, C., "Free Convection Melting in Ice Sphere," AIChE. J., Vol. 16, 1970, pp. 76-82.
10. Sparrow, E.M., Schmidt, R.R., and Ramsey, J.W., "Experiments on the Role of Natural Convection in the Melting of Solids," ASME J. Heat Trans., Vol. 100, 1978, pp. 11-16.
11. Sparrow, E.M., Ramsey, J.W., and Kemink, R.G., "Freezing Controlled by Natural Convection," ASME J. Heat Trans., Vol. 101, 1979, pp. 578-584.
12. Bareiss, M. and Beer, H., "Influence of Natural Convection on the Melting Process in a Vertical Cylinder Enclosure," Letters in Heat Mass Trans., Vol. 7, 1980, pp. 329-338.
13. Yao, L.S. and Chen, F.F., "Effects of Natural Convection in the Melted Region Around a Heated Horizontal Cylinder," ASME J. Heat Trans., Vol. 12, 1980, pp. 667-672.
14. Ramachandran, N., Gupta, J.P. and Jaluria, Y., "Thermal and Fluid Flow Effects During Solidification in a Rectangular Enclosure," Int. J. Heat Mass Trans., Vol. 25, 1982, pp. 187-193.

15. Ramachandran, N., Gupta, J.P., and Jaluria, Y., "Two-Dimensional Solidification with Natural Convection in the Melt and Convective and Radiative Boundary Conditions," Numer. Heat Trans., Vol. 4, 1981, pp. 469-484.
16. Gadgil, A. and Gobin, D., "Analysis of Two-Dimensional Melting in Rectangular Enclosure in Presence of Convection," ASME J. Heat Trans., Vol. 106, 1984, pp. 20-26.
17. Kroeger, P.G. and Ostarch, S., "The Solution of a Two-Dimensional Freezing Problem Including Convection," Int. J. Heat Mass Trans., Vol. 17, 1974, pp. 1191-1207.
18. Ockenden, J.R. and Hodgkins, W.R. (eds.), Moving Boundary Problems in Heat Flow and Diffusion, Clarendon, Oxford, 1977
19. Wilson, D.G., Solomon, A.D. and Boggs, P.T. (eds.), Moving Boundary Problems, Academic Press, New York, 1978.
20. Comini, G. and Del Giudice, S., "Finite Element Solutions of Non-linear Heat Conduction Problems with Special Reference to Phase Change," Int. J. Numer. Methods Eng., Vol. 8, pp. 613-624, 1979.
21. Ronel, J. and Baliga, B.R., "A Finite Element Method for Unsteady Heat Conduction in Materials with or without Phase Change," ASME Pap. 79-WA/HT-54, 1979.
22. Bonnerot, R. and Janet, P., "Numerical Computation of the Free Boundary for the Two-dimensional Stefan Problem by Space-Time Finite Elements," J. Comput. Phys., Vol. 25, pp. 163-181, 1977.
23. Lynch, D.R. and O'Neill, K., "Continuously Deforming Finite Elements for the Solution of Parabolic Problems with and without Phase Change," Int. J. Numer. Methods Eng., Vol. 17, pp. 81-96, 1981.
24. Desai, C.S., "Finite Element Methods for Flows in a Porous Media," in Finite Elements in Fluids, R.H. Gallagher et al. (eds.), Chap. 8, Wiley, London, 1975.
25. Miller, K. and Miller, R.N., "Moving Finite Elements, SIAM J. Numer. Anal., Vol. 18, pp. 1019-1033, 1981.
26. Rubinsky, B. and Cravalho, E.G., "A Finite Element Method for the Solution of One-Dimensional Phase Change Problems," Int. J. Heat Mass Transfer, Vol. 24, pp. 1987-1989, 1981.
27. Rubinsky, B., "Solidification Processes in Saline Solutions," ASME Pap. 82-WA/HT-13, 1982.
28. Yoo, J. and Rubinsky, B., "Numerical Computation Using Finite Elements for the Moving Interface in Heat Transfer Problems with Phase Transformation," Numerical Heat Transfer, Vol. 6, pp. 209-222, 1983.
29. Rubinsky, B. and Yoo, J., "Solid-Liquid Interface Morphology During Transient Solidification Processes in Undercooled Liquids," submitted for publication, J. of Heat Transfer, ASME Trans.

30. Bathe, K.J. and Wilson, E.L., "Numerical Methods in Finite Element Analysis, Prentice-Hall, England Cliff, N.J., 1976.
31. Backer, E.B., Corey, G.F., and Oden, J.J., "Finite Elements," Vol. I, Prentice-Hall, England Cliff, N.J. 1981.
32. Huebner, K.H. and Thornton, E.A., "The Finite Element Method for Engineering," 2nd ed., Wiley, N.Y., 1982.
33. Chung, T.J., "Finite Element Analysis in Fluid Dynamics," McGraw-Hill, N.Y., 1978.
34. Courant, R., Friedrichs, K., and Lewy, J., "Uber die Partieller Differenzgleichungen der Mathematischen Physik," Mathematische Annalen, Vol. 100, 1928, p. 32.
35. Babuska, I., "The Finite Element Method with Penalty," Tech. Note BN-710, The Institute for Fluid Dynamics and Applied Mathematics, University of Maryland, August 1971.
36. Zienkiewicz, O.C., "Constrained Variational Principles and Penalty Function Methods in Finite Element Analysis," Lecture Notes in Mathematics: Conference on the Numerical Solution of Differential Equations, edited by G.A. Watson, Springer-Verlag, Berlin, 1974, pp. 207-214.
37. Reddy, J.N., "On the Finite Element Model with Penalty for Incompressible Fluid Flow Problems," The Mathematics of Finite Elements and Applications III, edited by J.R. Whiteman, Academic Press, London, 1979, pp. 227-235.
38. Oden, J.T. and Jacqotte, O., "A Stable Second-Order Accurate, Finite Element Scheme for the Analysis of Two-Dimensional Incompressible Viscous Flows," Proc. 4th Int. Symposium on Finite Elements in Flow Problems, Tokyo, Japan, 1983.
39. Reddy, J.N., "The Penalty Function Method in Mechanics: A Review of Recent Advances," ASME AMD, Vol. 52, 2983, pp. 1-20.
40. Oden, J.T., "Penalty Method and Reduced Integration for the Analysis of Fluids," ASME AMD, Vol. 51, 1982, pp. 21-32.
41. Kheshgi, H.S. and Scriven, L.E., "Finite Element Analysis of Incompressible Viscous Flow by a Variable Penalty Function Method," ASME AMD, Vol. 51,
42. Zienkiewicz, O.C., "The Finite Element Method in Engineering Science," McGraw-Hill, London, 1971.
43. Marshall, R.S. Heinrich, J.C., and Zienkiewicz, O.C., "Natural Convection in a Saure Enclosure by a Finite-Element, Penalty Function Method Using Primitive Variables," Numer. Heat Trans. Vol. 1, 1978, pp. 315-330.

Table 1
Thermal Properties of Aluminum

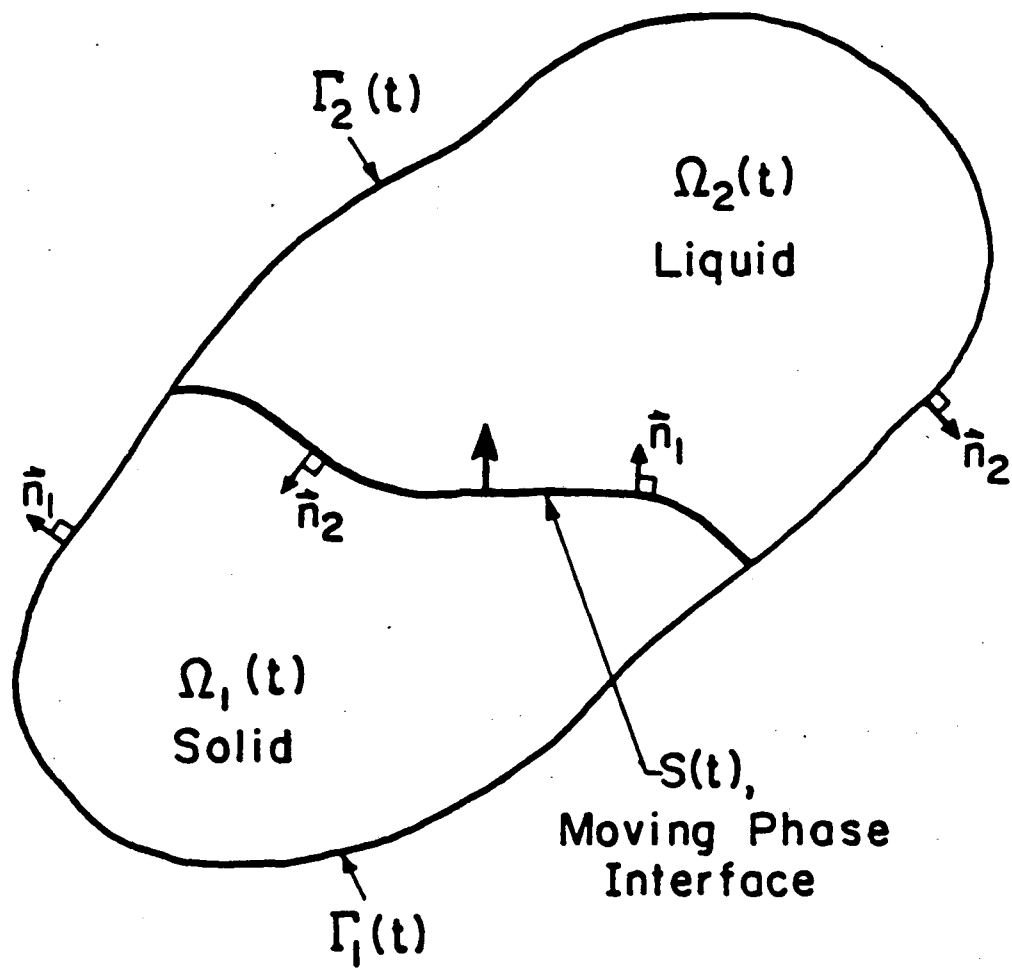
	solid	liquid	units
k	0.597	0.239	cal/cm sec °C
c_p	0.215	0.259	cal/g °C
H_{si}	95.0	95.0	cal/g
ρ	2.52	2.52	g/cm ³
T_m	660	660	°C
α	1.102	0.3662	cm ² /sec

Table 2
Dimensionless Parameters for Aluminum

Group	definition	value
Rayleigh number	$Ra = \beta g(T_i - T_m)L^3/\alpha_2\nu$	$10^2 - 10^5$
Prandtl number	$Pr = \nu/\alpha_2$	0.03041
Ratio		
Conductivity		2.4979
Therrmal diffusivity	$R_a = \alpha_1/\alpha_2$	3.0093
Biot number	$Bi = hL/k_1$	1.1357 - 3.4071
Stefan number		
solid	$Ste_1 = c_{p1}(T_i - T_m)/H_{si}$	0.6809 - 1.3619
liquid	$Ste_2 = c_{p2}(T_i - T_m)/H_{si}$	0.2726 - 0.5452

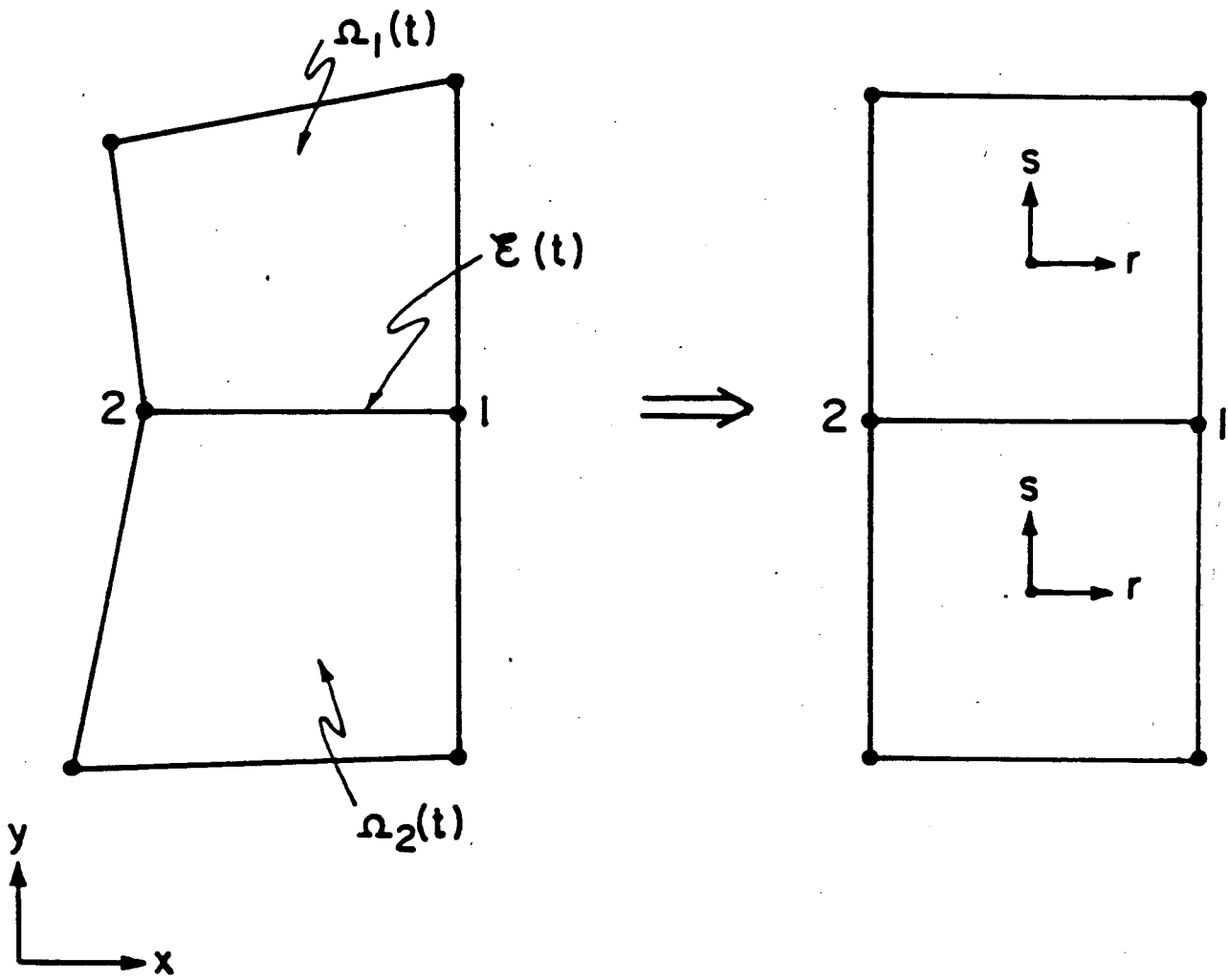
List of Figures

- Fig. 1 Schematic of the domain of discussion.
- Fig. 2 Schematic of a two-element domain.
- Fig. 3 Vector plot of the velocity field for $Ra = 10^5$, $H = 1.0$, $\theta_\infty = -3$, and $t^* = 0.025$.
- Fig. 4 Vector plot of the velocity field for $Ra = 10^5$, $H = 1.0$, $\theta_\infty = -3$, and $t^* = 0.05$.
- Fig. 5 Vector plot of the velocity field for $Ra = 10^5$, $H = 1.0$, $\theta_\infty = -3$, and $t = 0.07$.
- Fig. 6 Isothermal lines for $Ra = 10^5$, $H = 1.0$, $\theta_\infty = -3$ and $t^* = 0.025$.
- Fig. 7 Isothermal lines for $Ra = 10^5$, $H = 1.0$, $\theta_\infty = -3$ and $t^* = 0.05$.
- Fig. 8 Isothermal lines for $Ra = 10^5$, $H = 1.0$, $\theta_\infty = -3$ and $t^* = 0.07$.
- Fig. 9 The movement of the interface for $Ra = 10^4; 10^5$, $H = 1.0$, $\theta_\infty = -3$.
- Table 1 Thermal properties of aluminum.
- Table 2 Dimensionless parameters for aluminum.



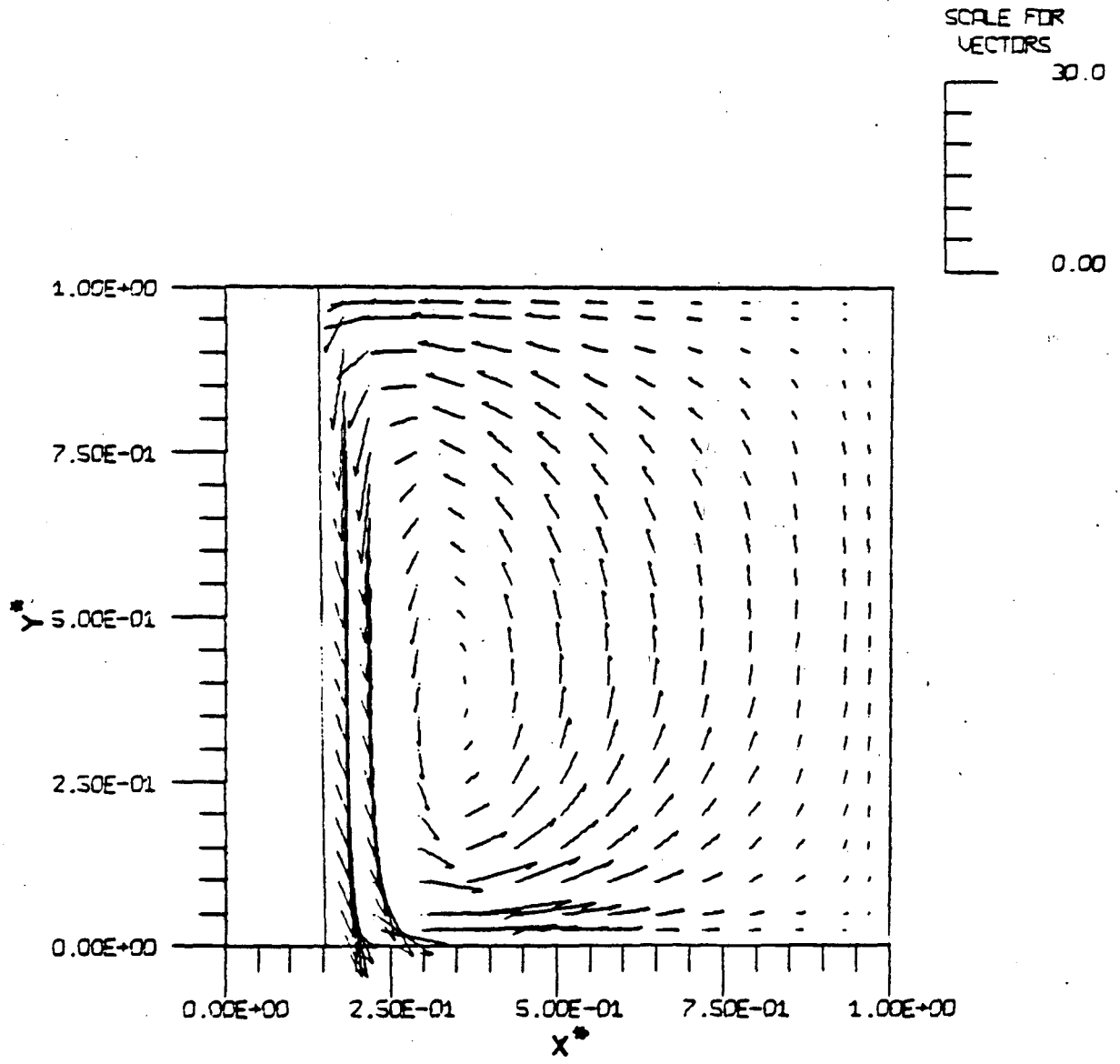
XBL 852-5839

Fig. 1



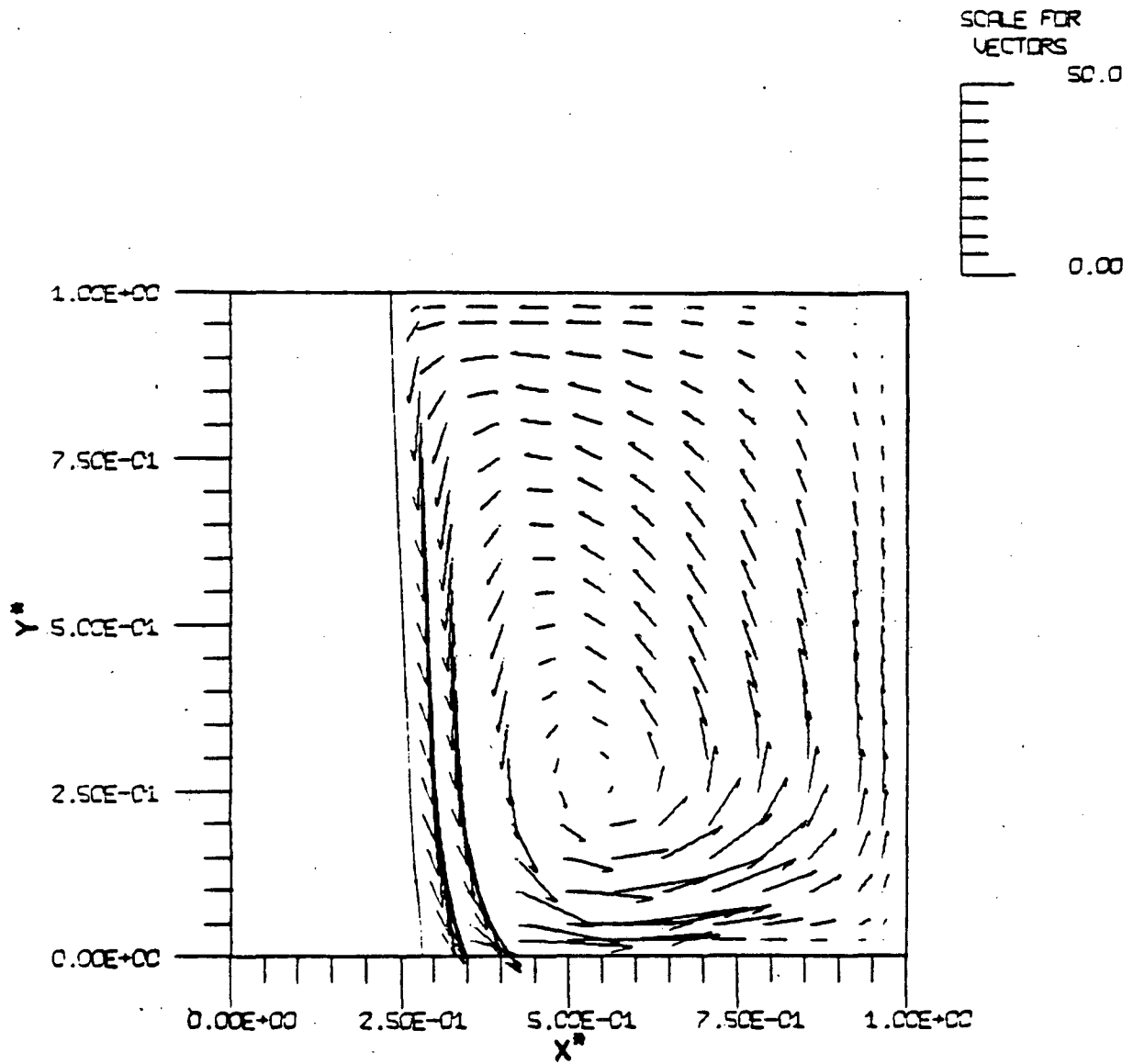
XBL 852-5847

Fig. 2



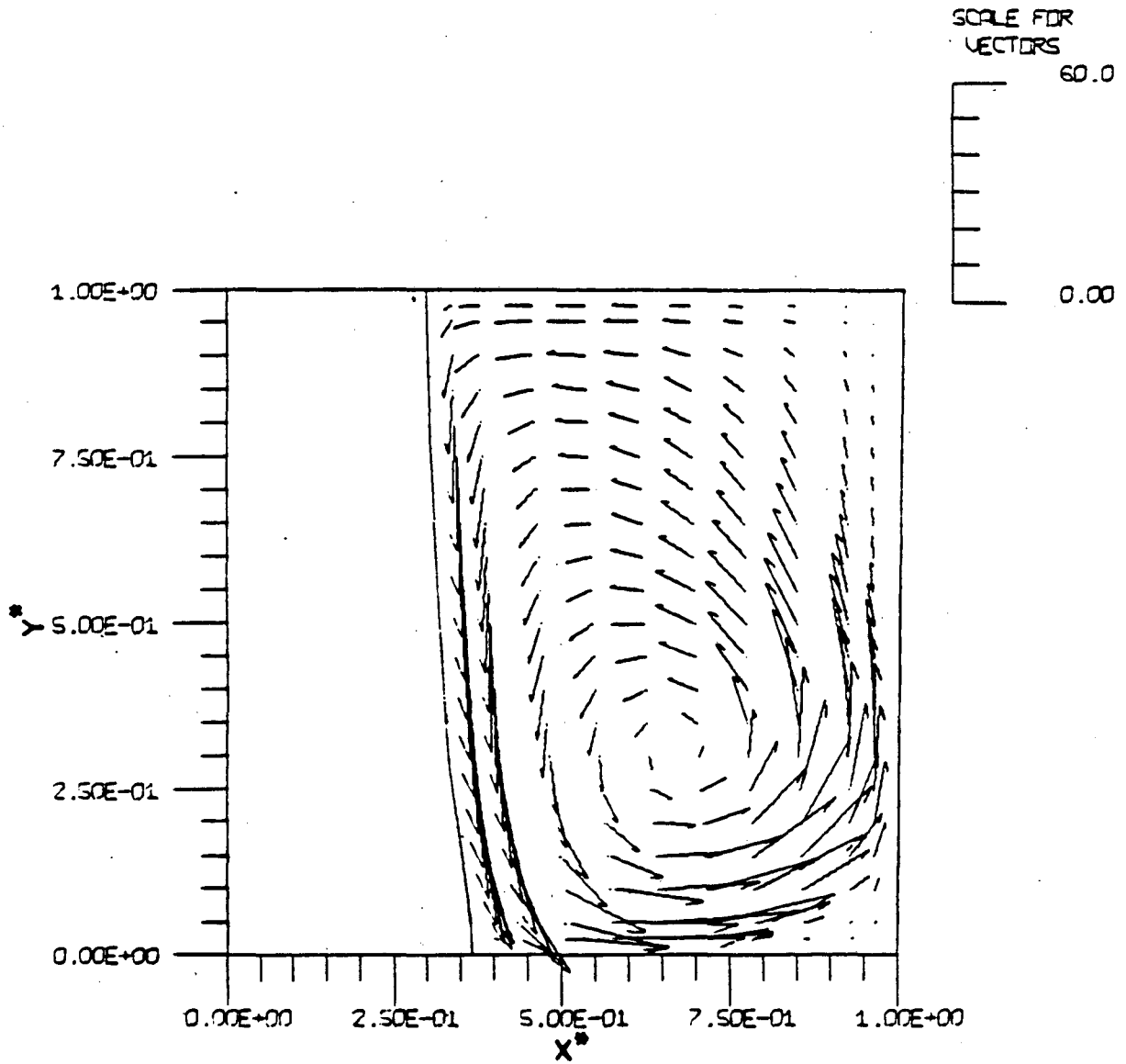
ABL 852-5846

Fig. 3



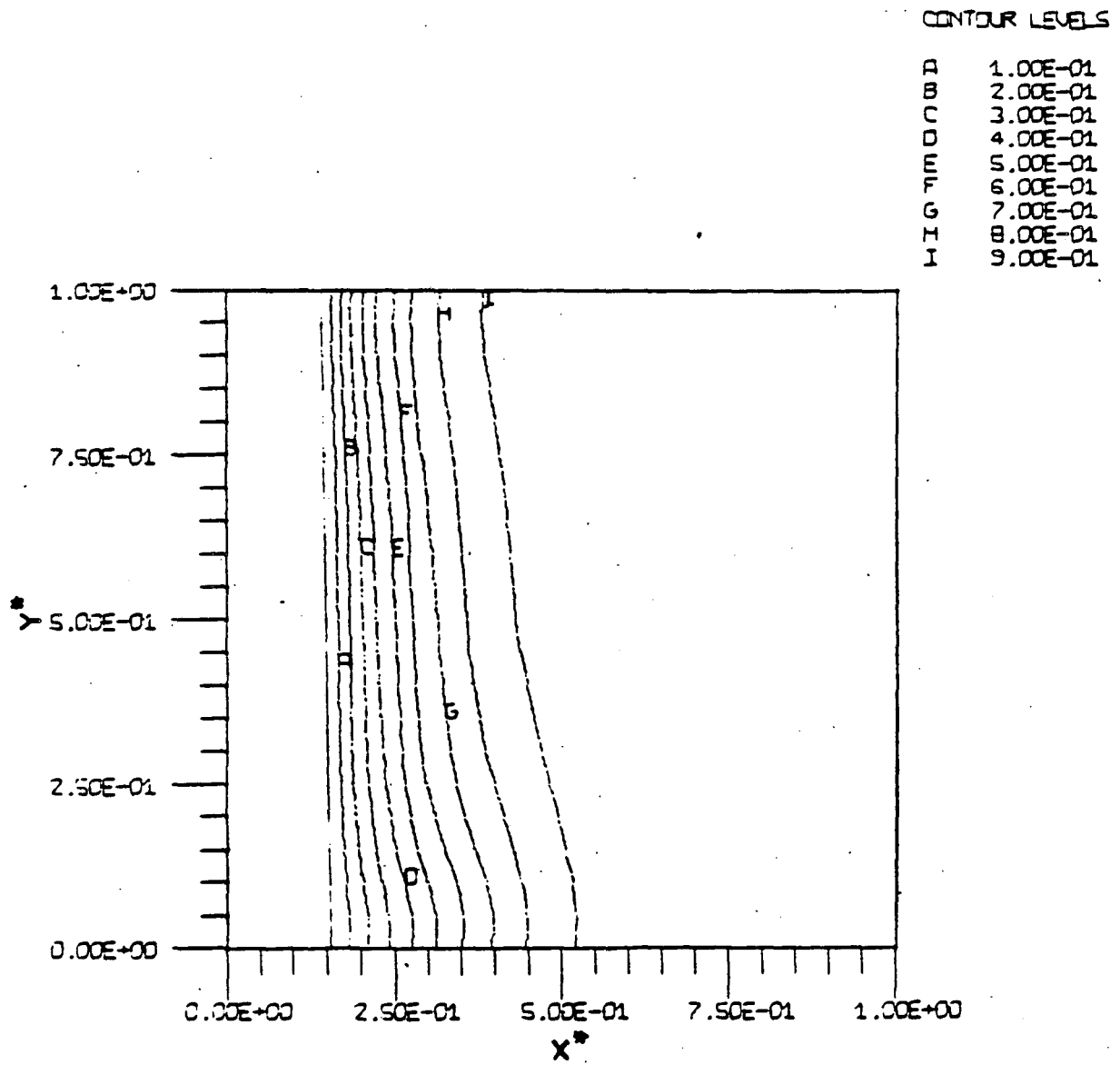
XBL852-5845

Fig. 4



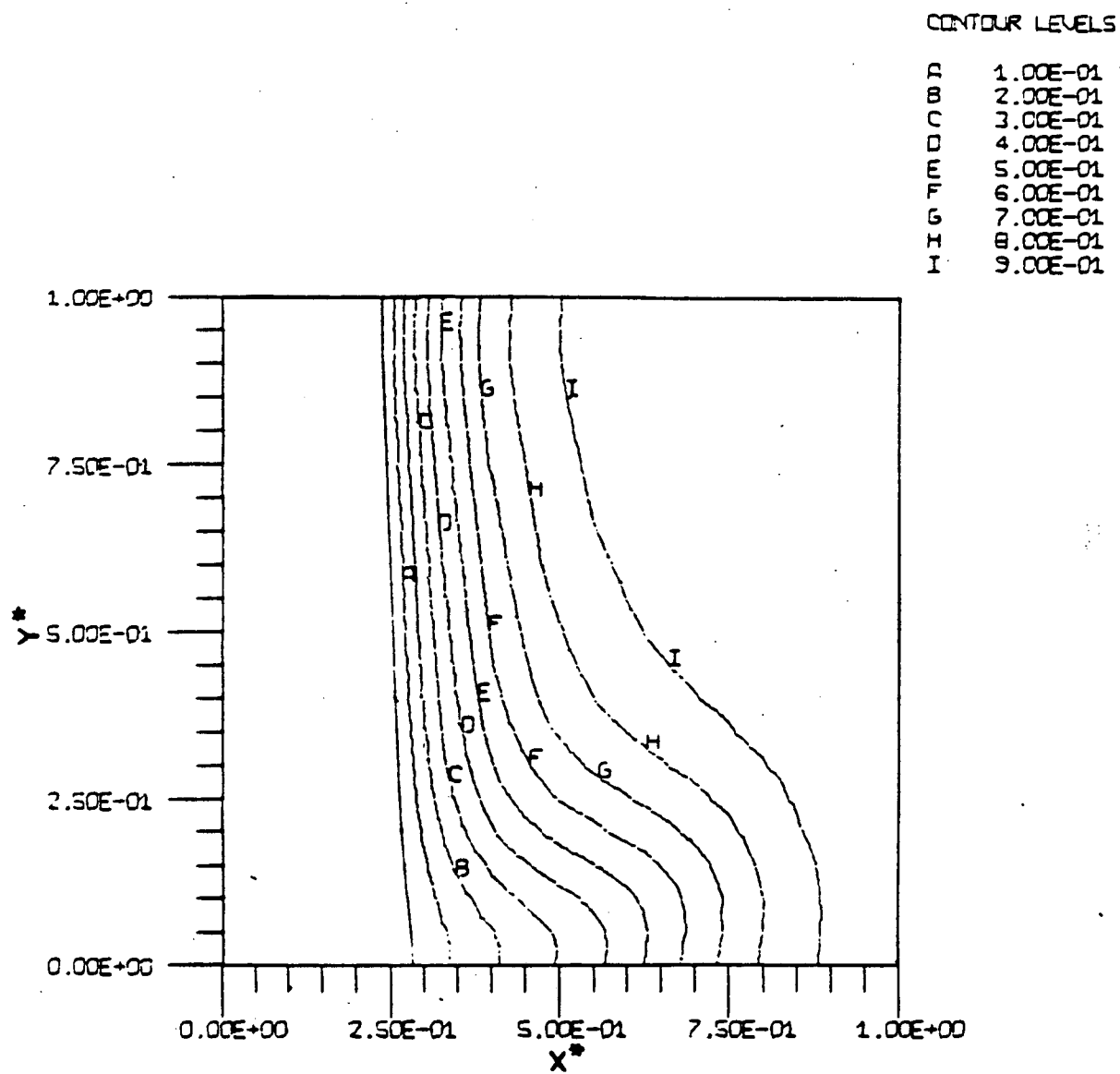
XBL 852-5844

Fig. 5



XBL852-5843

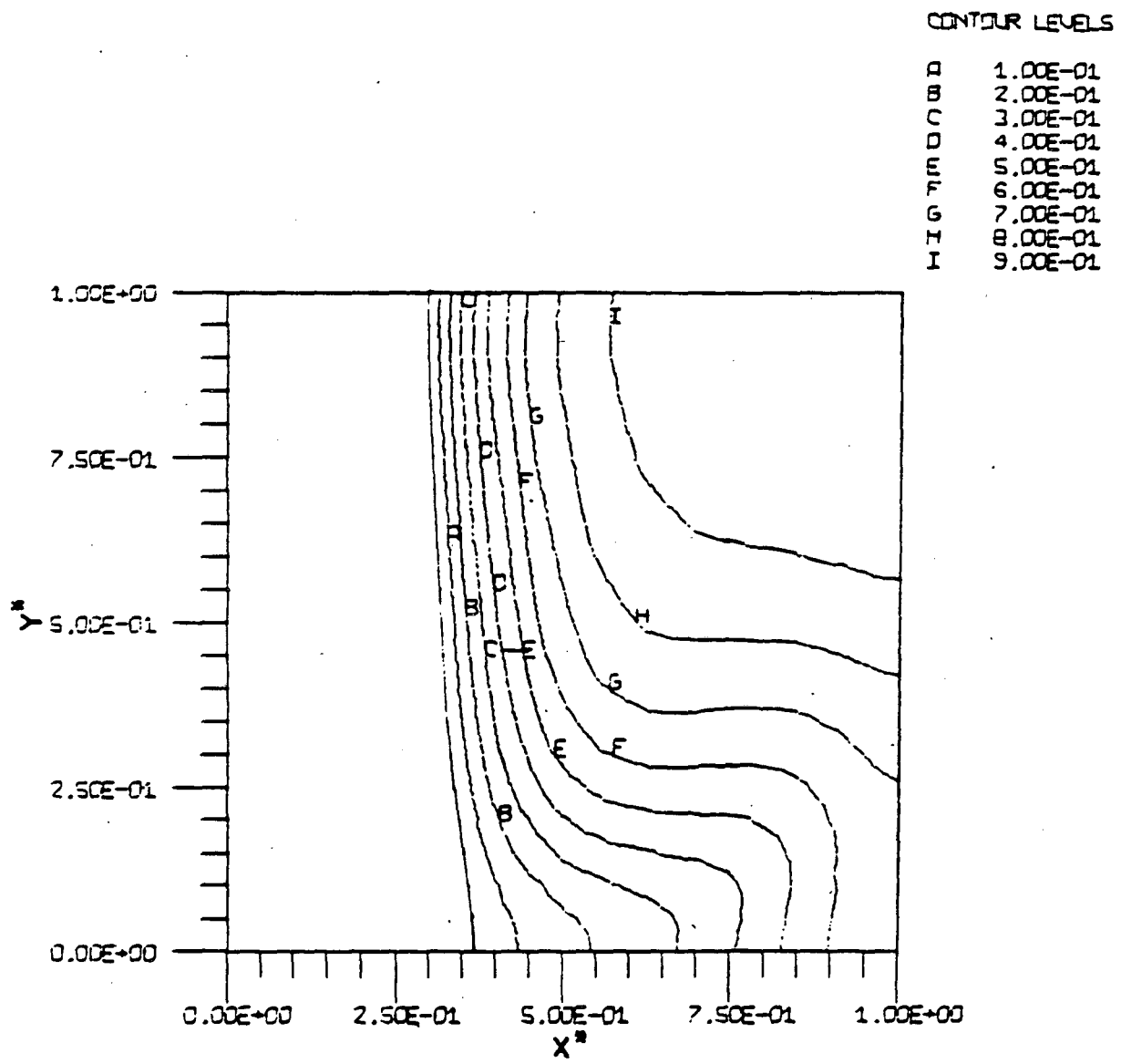
Fig. 6



XBL852-5842

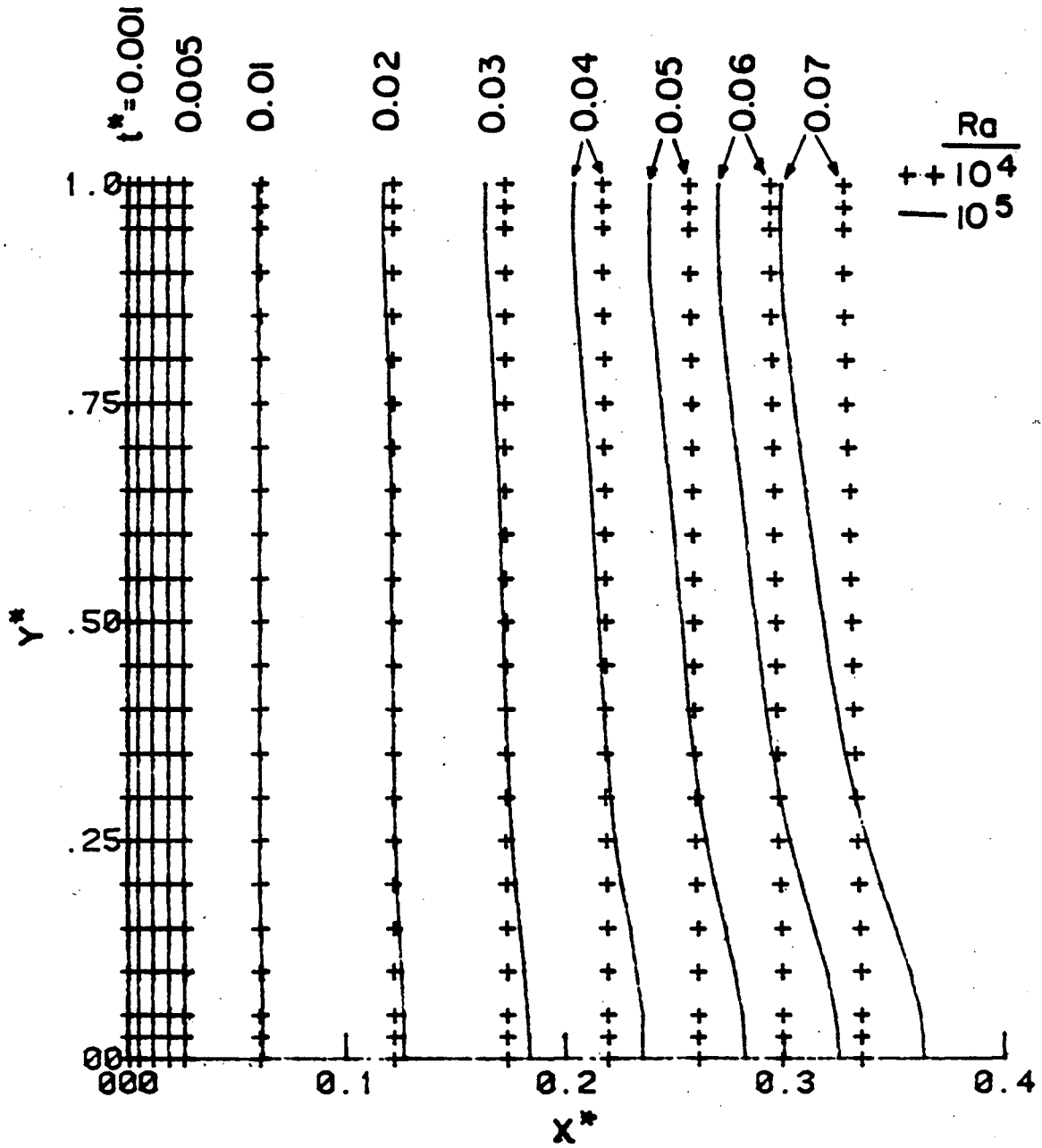
Fig. 7

Fig 8



XBL 852-5841

Fig. 8



XBL 852-5840

Fig. 9

This report was done with support from the Department of Energy. Any conclusions or opinions expressed in this report represent solely those of the author(s) and not necessarily those of The Regents of the University of California, the Lawrence Berkeley Laboratory or the Department of Energy.

Reference to a company or product name does not imply approval or recommendation of the product by the University of California or the U.S. Department of Energy to the exclusion of others that may be suitable.

TECHNICAL INFORMATION DEPARTMENT
LAWRENCE BERKELEY LABORATORY
UNIVERSITY OF CALIFORNIA
BERKELEY, CALIFORNIA 94720